Vol. 2, No. 1, June 2018
ISSN: 2616-1303 | **Web:** *www.cjpas.fulokoja.edu.ng*

FLOW OF AN ELECTRICALLY CONDUCTING NANOFLUID OVER A SEMI-INFINITE VERTICAL POROUS PLATE WITH SORET-DUFOUR EFFECTS

Idowu A.S.[a], Falodun, B.O.[b,*]
[a,b]Faculty of Physical Sciences, Department of Mathematics,
University of Ilorin, Kwara State, Nigeria.
Corresponding author:[a]asidowu@gmail.com,
[b,*]falodunbidemi2014@gmail.com

ABSTRACT
The mathematical model of electrically conducting Nanofluid flow over a semi-infinite vertical porous plate with Soret-Dufour effects is considered. The partial differential equations were non-dimensionalized via non-dimensional quantities and solved numerically using spectral relaxation method. Numerical computations of all flow parameters and physical quantities of engineering interest are presented in graphs and tables. The result shows that both Soret and Dufour parameter increases the velocity profile. The solutal boundary layer decreases because of the destructive chemical reaction

1.0.Introduction
Heat with mass transfer in Nanofluids has wide range of applications, and plays a significant role in sciences and engineering. A nanofluid contains a base fluid and nanoparticles. Investigations have shown that nanofluids enhance the thermal conductivity as well as the convective heat transfer performance of the base fluids. This enhancement is caused majorly by the Brownian motions of the nanoparticles inside the base fluids. Nanofluid is the suspension of nano-sized particles in the base fluid. (Ramana et al. 2016) found out that spherical shaped nanoparticles have effective thermal conductivity more than the cylindrical shaped nanoparticles. (Das 2015) studied the flow of nanofluid over a non-linear permeable stretching sheet with partial slip. The study concluded that nanoparticle concentration is an increasing function of each values of the slip and non-linear stretching parameter.(Ganga et al.2016) examined MHD flow of Boungiorno model nanofluid over a vertical plate. Homotopy analysis method was used in solving their model equations and they found out that increasing the controlling flow parameters increases the nanofluid temperature profile. (Misra and Adhikary2016) studied MHD oscillatory channel flow, heat and mass transfer in a physiological fluid with chemical reaction. Their study revealed that reduction in mass diffusivity enhances the mass transfer rate. The recent study of (Durga et al. 2018) on analysis of heat and mass transfer for MHD flow of nanofluid concluded that velocity of the fluid decreases with increasing values of magnetic and suction parameter for both nanoparticles

***Corresponding Author**
How to cite this paper: Idowu A.S., Falodun, B.O. (2018).
Flow of an electrically conducting nanofluid over a semi-infinite vertical porous plate with soret-dufour effects.
Confluence Journal of Pure and Applied Sciences (CJPAS), 2(1), 198 - 207.

Vol. 2, No. 1, June 2018
ISSN: 2616-1303 | **Web:** *www.cjpas.fulokoja.edu.ng*

$$\frac{\partial \bar{v}}{\partial \bar{y}} = 0 \quad (1)$$

$$\frac{\partial \bar{u}}{\partial \bar{t}} + \bar{v}\frac{\partial \bar{u}}{\partial \bar{y}} = \nu\frac{\partial^2 \bar{u}}{\partial \bar{y}^2} + g\beta(T - T_\infty) + g\beta^*(C - C_\infty) - \frac{\sigma\beta_0^2}{\rho}\bar{u} - \frac{\nu}{K}\bar{u} \quad (2)$$

$$\frac{\partial T}{\partial \bar{t}} + \bar{v}\frac{\partial T}{\partial \bar{y}} = \alpha\frac{\partial^2 T}{\partial \bar{y}^2} - \frac{1}{\rho c_p}\frac{\partial q_r}{\partial \bar{y}} + \frac{\mu}{\rho c_p}\left(\frac{\partial \bar{u}}{\partial \bar{y}}\right)^2 + \frac{Dk_T}{c_s c_p}\frac{\partial^2 C}{\partial \bar{y}^2} + \frac{Q_0}{\rho c_p}(T - T_\infty)$$

$$+\tau^*\left[D_B\frac{\partial C}{\partial \bar{y}}\frac{\partial T}{\partial \bar{y}} + \frac{D_T}{T_\infty}\left(\frac{\partial T}{\partial \bar{y}^2}\right)^2\right] \quad (3)$$

$$\frac{\partial C}{\partial \bar{t}} + \bar{v}\frac{\partial C}{\partial \bar{y}} = D\frac{\partial^2 C}{\partial \bar{y}^2} - K_r'^2(C - C_\infty) + \frac{Dk_T}{T_m}\frac{\partial^2 T}{\partial \bar{y}^2} \quad (4)$$

subject to

$$\bar{u} = u_0,\ T = T_w + \psi(T_w - T_\infty)e^{\bar{n}\bar{t}},\ C = C_w + \psi(C_w - C_\infty)e^{\bar{n}\bar{t}}$$

$$D_B\frac{\partial C}{\partial \bar{y}} + \frac{D_T}{T_\infty}\frac{\partial T}{\partial \bar{y}} = 0, \quad at \quad \bar{y} = 0 \quad (5)$$

$$\bar{u} \to 0, \quad T \to T_\infty, \quad C \to C_\infty \quad as \quad \bar{y} = \infty \quad (6)$$

Where $\bar{u}$ and $\bar{v}$ are the velocity components in $\bar{x}$ and $\bar{y}$ direction respectively, T is the fluid temperature, C is the fluid dimensionless concentration, $\bar{t}$ is the time, c_p is the specific heat at constant pressure, D is the mass diffusivity, g is the acceleration due to gravity, β and β^* are the thermal expansion and concentration expansion coefficient respectively, σ is the electrical conductivity of the fluid, β_0 is the external imposed magnetic field strength in the y direction, ρ is the fluid density, ν is the fluid viscosity, K is the porosity term, α is the fluid thermal diffusivity, q_r is the radiative heat flux, c_s is the concentration susceptivity, k_T is the thermal diffusion ratio, Q_0 is the heat generation parameter, T_∞ and C_∞ are the free stream temperature and concentration respectively, D_B is the Brownian diffusion coefficient, K_r' is the chemical reaction parameter, T_w and C_w are wall temperature and concentration respectively, $\bar{n}$ is a constant.

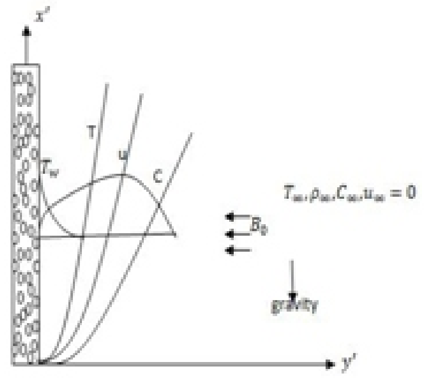

Figure 1: Physical interpretation of the Problem

Considering the Rosseland diffusion approximation (Hossain *et al.*, 1999) and following published work of (Idowu and Falodun 2019) and (Adegbie and Fagbade 2015), the radiative heat flux is given by

$$q_r = -\frac{4\sigma_0}{3k_s}\frac{\partial T^4}{\partial \bar{y}} \quad (7)$$

Assuming that the temperature differences within the boundary layer flow are sufficiently small in a way that T^4 in eqn (7) may be expressed as a linear function of temperature.

$$T^4 \cong 4T_\infty^3 T - 3T_\infty^4 \quad (8)$$

Substituting eqn (7) and (8) into (3) to obtain

$$\frac{\partial T}{\partial \bar{t}} + \bar{v}\frac{\partial T}{\partial \bar{y}} = \alpha\frac{\partial^2 T}{\partial \bar{y}^2} + \frac{16\sigma_0 T_\infty^3}{3k_s\rho c_p}\frac{\partial^2 T}{\partial \bar{y}^2} + \frac{\mu}{\rho c_p}\left(\frac{\partial \bar{u}}{\partial \bar{y}}\right)^2 + \frac{Dk_T}{c_s c_p}\frac{\partial^2 C}{\partial \bar{y}^2} + \frac{Q_0}{\rho c_p}(T - T_\infty)$$

$$+\tau^*\left[D_B\frac{\partial C}{\partial \bar{y}}\frac{\partial T}{\partial \bar{y}} + \frac{D_T}{T_\infty}\left(\frac{\partial T}{\partial \bar{y}^2}\right)^2\right] \quad (9)$$

Integrating both sides of the continuity eqn (1) to obtain the suction velocity normal to the plate. In this paper, the suction velocity normal to the plate is considered to be constant and time dependent as given by Idowu and Falodun (2018)

$$\bar{v} = V_0(1 + \epsilon A e^{\bar{n}\bar{t}}) \quad (10)$$

For the equations of motion in eqn (2)-(4) subject to (5) and (6) to be writing in dimensionless form, the following non-dimensional quantities are introduced:

Vol. 2, No. 1, June 2018
ISSN: 2616-1303 | **Web:***www.cjpas.fulokoja.edu.ng*

$$u=\frac{\bar{u}}{u_0},\quad y=\frac{v_0^2\bar{y}}{\upsilon},\frac{v_0^2\bar{t}}{\upsilon},\quad n=\frac{\upsilon\bar{n}}{v_0^2}$$

$$\theta=\frac{T-T_\infty}{T_w-T_\infty},\quad \phi=\frac{C-C_\infty}{C_w-C_\infty} \qquad (11)$$

Applying the above eqn (11) into (2)-(4) subject to (5) and (6) leads to:

$$\frac{\partial u}{\partial t}-(1+\epsilon Ae^{nt})\frac{\partial u}{\partial y}=\frac{\partial^2 u}{\partial y^2}+G_t\theta+G_m\phi-\left(M+\frac{1}{Ps}\right)u \qquad (12)$$

$$\frac{\partial\theta}{\partial t}-(1+\epsilon Ae^{nt})\frac{\partial\theta}{\partial y}=\left(\frac{1+Rd}{Pr}\right)\frac{\partial^2\theta}{\partial y^2}+Ec\left(\frac{\partial u}{\partial y}\right)^2+D_0\frac{\partial^2\phi}{\partial y^2}+Hg\theta+Nb\frac{\partial\phi}{\partial y}\frac{\partial\theta}{\partial y}+N_t\left(\frac{\partial\theta}{\partial y}\right)^2 \qquad (13)$$

$$\frac{\partial\phi}{\partial t}-(1+\epsilon Ae^{nt})\frac{\partial\phi}{\partial y}=\frac{1}{Sc}\frac{\partial^2\phi}{\partial y^2}-K_c\phi+\left(\frac{SoLnNb+N_t}{LnNb}\right)\frac{\partial^2\theta}{\partial y^2} \qquad (14)$$

Subject to the initial and boundary conditions

$$u=1,\ \theta=1+\epsilon e^{nt},\ \phi=1+\epsilon e^{nt},\frac{\partial\phi}{\partial y}+\frac{N_t}{Nb}\frac{\partial\theta}{\partial y}=0\quad at\quad y=0 \qquad (15)$$

$$u\to 0,\ \theta\to 0,\ \phi\to 0,\quad at\quad y\to\infty \qquad (16)$$

Where

$$G_t=\frac{g\beta_t\nu(T_w-T_\infty)}{u_0v_0^2},Gm=\frac{g\beta_c\nu(C_w-C_\infty)}{u_0v_0^2},M=\frac{\sigma\beta_0^2\nu}{\rho u_0v_0},Ps=\frac{Ku_0v_0}{\nu\nu},Rd=\frac{16\sigma_0T_\infty^3}{3K_e\nu},Pr=\frac{\rho c_p}{k},Ec=\frac{\mu v_0^2}{\rho c_p\nu(T_w-T_\infty)},\ D_0=\frac{Dk_T(C_w-C_\infty)}{c_sc_p(T_w-T_\infty)},Hg=\frac{Q_0\nu}{\rho c_pv_0^2},Nb=\frac{\tau D_B(C_w-C_\infty)}{\nu},\ N_t=\frac{\tau D_T(T_w-T_\infty)}{T_\infty\nu},Ln=\frac{\nu}{D_B},$$

$$Sc=\frac{\nu}{D},K_c=\frac{K_r'^2\nu}{v_0^2}$$

are the thermal Grashof number, mass Grashof number, magnetic parameter, permeability parameter, radiation parameter, Prandtl number, Eckert number, Dufour number, heat generation parameter, Brownian motion parameter, thermophoresis parameter, Lewis number, Schmidt number and chemical reaction parameter respectively.

3.0Methodology

The spectral relaxation analysis (SRM) is used in this section to solve the dimensionalized system of partial differential equations iterative. It employs the Gauss-siedel approach of relaxation to simultaneously linearrize and decoupled the transformed coupled differential equations. Chebyshev pseudo-spectral method is used further to discretize and solve the resulting equations. $r+1$ is used to denoted the linear terms in each equation and are evaluated at the current iteration level while the non-linear terms denoted by r is assumed to be known from the previous iteration level. Applying SRM, the resulting differential equations are first re-arranged and decoupled using the systematic approach of Gauss-siedel.

$$\frac{\partial u}{\partial t}=\frac{\partial^2 u}{\partial y^2}+(1+\epsilon Ae^{nt})\frac{\partial u}{\partial y}+G_t\theta+G_m\phi-\left(M+\frac{1}{Ps}\right)u \qquad (17)$$

$$\frac{\partial\theta}{\partial t}=\left(\frac{1+Rd}{Pr}\right)\frac{\partial^2\theta}{\partial y^2}+(1+\epsilon Ae^{nt})\frac{\partial\theta}{\partial y}+Ec\left(\frac{\partial u}{\partial y}\right)^2+D_0\frac{\partial^2\phi}{\partial y^2}+Hg\theta+Nb\frac{\partial\phi}{\partial y}\frac{\partial\theta}{\partial y}+N_t\left(\frac{\partial\theta}{\partial y}\right)^2 \qquad (18)$$

$$\frac{\partial\phi}{\partial t}=\frac{1}{Sc}\frac{\partial^2\phi}{\partial y^2}+(1+\epsilon Ae^{nt})\frac{\partial\phi}{\partial y}-K_c\phi+\left(\frac{SoLnNb+N_t}{LnNb}\right)\frac{\partial^2\theta}{\partial y^2} \qquad (19)$$

subject to the initial and boundary conditions

$$u=1,\ \theta=1+\epsilon e^{nt},\ \phi=1+\epsilon e^{nt},\frac{\partial\phi}{\partial y}+\frac{N_t}{Nb}\frac{\partial\theta}{\partial y}=0\quad at\quad y=0 \qquad (20)$$

$$u\to 0,\ \theta\to 0,\ \phi\to 0,\quad at\quad y\to\infty \qquad (21)$$

Applying SRM on (17)-(19) subject to (20) and (21) leads to:

$$\frac{\partial u_{r+1}}{\partial t}=\frac{\partial^2 u_{r+1}}{\partial y^2}+(1+\epsilon Ae^{nt})\frac{\partial u_{r+1}}{\partial y}+G_t\theta_r+G_m\phi_r-\left(M+\frac{1}{Ps}\right)u_{r+1} \qquad (22)$$

$$\frac{\partial\theta_{r+1}}{\partial t}=\left(\frac{1+Rd}{Pr}\right)\frac{\partial^2\theta_{r+1}}{\partial y^2}+(1+\epsilon Ae^{nt})\frac{\partial\theta_{r+1}}{\partial y}+Ec\left(\frac{\partial u_{r+1}}{\partial y}\right)^2+D_0\frac{\partial^2\phi_r}{\partial y^2}+Hg\theta_{r+1}+Nb\frac{\partial\phi_r}{\partial y}\frac{\partial\theta_{r+1}}{\partial y}+N_t\left(\frac{\partial\theta_{r+1}}{\partial y}\right)^2$$

$$\frac{\partial\phi_{r+1}}{\partial t}=\frac{1}{Sc}\frac{\partial^2\phi_{r+1}}{\partial y^2}+(1+\epsilon Ae^{nt})\frac{\partial\phi_{r+1}}{\partial y}-K_c\phi_{r+1}+\left(\frac{SoLnNb+N_t}{LnNb}\right)\frac{\partial^2\theta_{r+1}}{\partial y^2} \qquad (24)$$

subject to:

$$u_{r+1}(y=0,t)=1.\theta_{r+1}(y=0,t)=1+$$

$\epsilon e^{nt}, \phi_{r+1}(y=0,t) = 1+\epsilon e^{nt}, \frac{\partial \phi_{r+1}}{\partial y} + \frac{N_t}{Nb}\frac{\partial \theta_{r+1}}{\partial y}, \; at \;\; y=0$

$$u_{r+1}(y=\infty,t)=0, \theta_{r+1}(y=\infty,t) = 0, \phi_{r+1}(y=\infty,t)=0 \quad at \quad y=\infty \qquad (26)$$

Let

$a_0 = (1+\epsilon e^{nt}), a_1 = G_t\theta_r + Gm\phi_r, \quad b_0 = (1+Rd), b_1 = Pr(\epsilon e^{nt}), b_2 = Ec\left(\frac{\partial u_{r+1}}{\partial y}\right)^2, b_3 = D_0\frac{\partial^2 \phi_r}{\partial y^2}$

$b_4 = Nb\frac{\partial \phi_r}{\partial y}, b_5 = N_t\left(\frac{\partial \theta_{r+1}}{\partial y}\right)^2, c_0 = LnNb, c_1 = ScLnNb(1+\epsilon e^{nt}), c_2 = Sc(SoLnNb + N_t)\frac{\partial^2 \theta_{r+1}}{\partial y^2}$

The substitution of the above coefficient parameters into (22)-(24) lead to:

$$\frac{\partial u_{r+1}}{\partial t} = \frac{\partial^2 u_{r+1}}{\partial y^2} + a_0\frac{\partial u_{r+1}}{\partial y} + a_1 - \left(M+\frac{1}{Ps}\right)u_{r+1} \qquad (27)$$

$$Pr\frac{\partial \theta_{r+1}}{\partial t} = b_0\frac{\partial^2 \theta_{r+1}}{\partial y^2} + b_1\frac{\partial \theta_{r+1}}{\partial y} + b_2 + b_3 + Hg\theta_{r+1} + b_4\frac{\partial \theta_{r+1}}{\partial y} + b_5 \qquad (28)$$

$$ScLnNb\frac{\partial \phi_{r+1}}{\partial y} = c_0\frac{\partial^2 \phi}{\partial y^2} + c_1\frac{\partial \phi_{r+1}}{\partial y} - ScK_cLnNb\phi_{r+1} + c_2 \qquad (29)$$

Subject to (25) and (26) The initial approximations $u_0(y,t), \theta_0(y,t)$ and $\phi_0(y,t)$ is chosen with respect to the boundary conditions (25) and (26) at $y=0$ as:

$$u_0(y,t) = e^{-y}, \theta_0(y,t) = \phi_0(y,t) = e^{-y} + \epsilon e^{nt}, (1-e^{-y})\frac{\partial \phi_{r+1}}{\partial y} + \frac{N_t}{Nb}\frac{\partial \theta_{r+1}}{\partial y} = 0 \qquad (30)$$

The schemes in (27), (28) and (29) are iteratively solved for $u_{r+1}(y,t), \theta_{r+1}(y,t)$ and $\phi_{r+1}(y,t)$ when $r=0,1,2$. The undetermined functions are defined with the Gauss-Lobatto point as

$$\xi_j = cos\frac{\pi_j}{N}, \quad j=0,1,2,\ldots,N; 1 \le \xi \le -1 \qquad (31)$$

In equation (31) above, N is the number of collocation points. At the physical region $[0,\infty]$ is transformed into $[-1,1]$. Therefore, the present problem is solved on the interval $[0,L]$ instead of $[0,\infty)$ by using $\frac{\eta}{L} = \frac{\xi+1}{2}$, $-1 \le \xi \le 1$ to map the interval together. L is the scalling parameter used as 30 in this paper to implement the boundary conditions to infinity. To solve (27)-(29), Chebyshev spectral collocation method is applied in y –direction. Also, implicit finite difference method is applied in t –direction. The finite difference scheme is applied with centering about a mid-point between t^{n+1} and t^n. The mid-point is given as $t^{n+\frac{1}{2}} = \frac{t^{n+1}+t^n}{2}$ and the centering about $t^{n+\frac{1}{2}}$ to the undetermined functions, say $u(y,t), \theta(y,t)$ and $\phi(y,t)$ and the derivative associating with it yield

$$u(y_j, t^{n+\frac{1}{2}}) = u_j^{n+\frac{1}{2}} = \frac{u_j^{n+1}+u_j^n}{2}, \left(\frac{\partial u}{\partial t}\right)^{n+\frac{1}{2}} = \frac{u_j^{n+1}-u_j^n}{\Delta t} \qquad (32)$$

$$\theta(y_j, t^{n+\frac{1}{2}}) = \theta_j^{n+\frac{1}{2}} = \frac{\theta_j^{n+1}+\theta_j^n}{2}, \left(\frac{\partial \theta}{\partial t}\right)^{n+\frac{1}{2}} = \frac{\theta_j^{n+1}-\theta_j^n}{\Delta t} \qquad (33)$$

$$\phi(y_j, t^{n+\frac{1}{2}}) = \phi_j^{n+\frac{1}{2}} = \frac{\phi_j^{n+1}+\phi_j^n}{2}, \left(\frac{\partial \phi}{\partial t}\right)^{n+\frac{1}{2}} = \frac{\phi_j^{n+1}-\phi_j^n}{\Delta t} \qquad (34)$$

Spectral collocation method requires the use of differentiation matrix D to approximate the derivatives of unknown variables given as

$$\frac{d^r u}{dy^r} = \sum_{k=0}^{N} D_{ik}^r u(\xi_k) = D^r u, \quad i=0,1,2,\ldots,N \qquad (35)$$

$$\frac{d^r \theta}{dy^r} = \sum_{k=0}^{N} D_{ik}^r \theta(\xi_k) = D^r \theta, \quad i=0,1,2,\ldots,N \qquad (36)$$

$$\frac{d^r \phi}{dy^r} = \sum_{k=0}^{N} D_{ik}^r \phi(\xi_k) = D^r \phi, \quad i=0,1,2,\ldots,N \qquad (37)$$

In eqns (35)-(37), r is the order of differentiation. Before the application of finite difference method on eqns (27)-(29), Chebyshev spectral collocation is first applied to obtain

$$\frac{du_{r+1}}{dt} = D^2u_{r+1} + a_0Du_{r+1} + a_1 - \left(M - \frac{1}{Ps}\right)u_{r+1} \qquad (38)$$

$$Pr\frac{d\theta_{r+1}}{dt} = b_0D^2\theta_{r=1} + b_1D\theta_{r+1} + b_2 + b_3 + Hg\theta_{r+1} + b_4D\theta_{r+1} + b_5 \qquad (39)$$

$$ScLnNb\frac{d\phi_{r+1}}{dt} = c_0D^2\phi_{r+1} + c_1D\phi_{r+1} - ScK_cLnNb\phi_{r+1} + c_2 \qquad (40)$$

subject to

$$u_{r+1}(x_0,t) = 1, u_{r+1}(xNx,t) = 0, \theta_{r+1}(x_0,t) = 1+\epsilon e^{nt}, \theta_{r+1}(xNx,t) = 0 \qquad (41)$$

$$\phi_{r+1}(x_0,t) = 1+\epsilon e^{nt}, \phi_{r+1}(xNx,t) = 0, \phi'_{r+1}(x_0,t) + \frac{N_t}{Nb}\theta'(x_0,t) = 0, \phi'_{r+1}(xNx,t) + \frac{N_t}{Nb}(xNx,t) = 0 \qquad (42)$$

Simplifying eqns (38)-(40) to yield

$$\beta_1 u_{r+1}^{n+1} = \beta_2 u_{r+1}^n + K_1 \qquad (43)$$

$$\alpha_1 \theta_{r+1}^{n+1} = \alpha_2 \theta_{r+1}^n + K_2 \qquad (44)$$

Vol. 2, No. 1, June 2018
ISSN: 2616-1303 | Web:www.cjpas.fulokoja.edu.ng

$$\gamma_1\phi_{r+1}^{n+1} = \gamma_2\phi_{r+1}^{n} + K_3 \quad (45)$$

Subject to:

$$u_{r+1}(xNx,t^n) = 0, \theta_{r+1}(xNx,t^n) = 0, \phi_{r+1}(xNx,t^n) = 0 \quad (46)$$

$$u_{r+1}(x_0,t^n) = 1, \theta_{r+1}(x_0,t^n) = \phi_{r+1}(x_0,t^n) = 1 + \epsilon e^{nt} \quad (47)$$

$$\left(\frac{\partial\phi}{\partial y} + \frac{N_t}{Nb}\frac{\partial\theta}{\partial y}\right)(xNx,t^n) = \left(\frac{\partial\phi}{\partial y} + \frac{N_t}{Nb}\frac{\partial\theta}{\partial y}\right)(x_0,t^n) = 0 \quad (48)$$

where $\beta_1, \beta_2, \alpha_1, \alpha_2, \gamma_1, \gamma_2, K_1, K_2$ and K_3 are matrices defined as:

$$\beta_1 = \frac{1}{\Delta t} - \frac{D^2 + a_0 D - \left(M + \frac{1}{Ps}\right)}{2}, \beta_2 = \frac{1}{\Delta t} + \frac{D^2 + a_0 D - \left(M + \frac{1}{Ps}\right)}{2}$$

$$\alpha_1 = \frac{Pr}{\Delta t} - \frac{b_0 D^2 + b_1 D + b_4 D + Hg}{2},$$

$$\alpha_2 = \frac{Pr}{\Delta t} + \frac{b_0 D^2 + b_1 D + b_4 D + Hg}{2}$$

$$\gamma_1 = \frac{ScLnNb}{Deltat} - \frac{c_0 D^2 + c_1 D - ScK_c LnNb}{2}, \gamma_2 = \frac{ScLnNb}{\Delta t} + \frac{c_0 D^2 + c_1 D - ScK_c LnNb}{2}$$

$$K_1 = a_{1,r}^{n+\frac{1}{2}}, K_2 = b_{2,r}^{n+\frac{1}{2}} + b_{3,r}^{n+\frac{1}{2}} + b_{5,r}^{n+\frac{1}{2}}, K_3 = c_{2,r}^{n+\frac{1}{2}}$$

4.0Results and Discussions

In the previous sections, the problem of unsteady heat and mass transfer in the presence of nano-particles was formulated and solved using SRM. The pictorial representation for velocity, temperature and concentration were obtained. Numeric values were obtained for the physical quantities such as skin friction (Cf), local Nusselt number (Nu) and sherwood number for various controlling parameters.

The temperature and the concentration fields are coupled with the velocity with thermal Grashof number and mass Grashof number. Also, the velocity and species concentration fields are coupled with temperature with Dufour term, brownian motion term and viscous dissipation term. Figure 2 represents the effect of Dufour term on the velocity, temperature and concentration profiles. It was noticed from figure 2 that diffusion thermal positively affects the fluid temperature and hereby accelerates the fluid temperature. The Dufour parameter increases the velocity profile as its value increases. This is due to great increase in the diffusion thermal as a result of increase in the Dufour parameter. The effect of Dufour parameter is negligible in the concentration profile. Figure 3 exibits the effect of Soret term (So) on the velocity, temperature and concentration profiles. So is seen to increase the velocity and concentration profiles within the boundary layer. The increase in the velocity is due to greater thermal diffusion. The concentration enhances when increasing the Soret parameter as shown in figure 3. The Soret parameter is seen to be negligible in figure 3 but increases the velocity profile. This is because, when So is increased, there will be greater thermal diffusion which results to increase in the fluid velocity. The effect of the thermal Grashof number (G_t) on the velocity, temperature and concentration profiles is illustrated in figure 4. It was noticed from figure 4 that the velocity overshot in the boundary layer. This is due to the buoyancy force which behaves like a pressure gradient. It accelerates the fluid within the boundary layer. Increase in the thermal Grashof number brings about rapid increase in the fluid velocity and decelerates to the free stream velocity. In addition, the temperature difference, that is $(T_w - T_\infty)$ increases with increase in Gr. However, the enhanced convection leads to the enhancement of velocity. Figure 5 depicts the effect of magnetic field parameter (M_p) on the velocity, temperature and concentration profiles. There is a damping effect on the flow velocity as a result of increase in magnetic parameter. Immediately currents are induced by motion of an electrically conducting fluid due to increase in magnetic field parameter a drag force acts on the fluid and reduces the fluid velocity. Increase in the Magnetic parameter (M_p) is seen in figure 5 to be negligible on the concentration profile.

The effect of heat generation parameter (Hg) on the velocity, temperature and concentration profiles is illustrated in figure 6. It was noticed that increase in the heat generation parameter (Hg) accelerates the fluid velocity. When heat is generated in the boundary layer, heat energy is produced and the boundary layer thickness becomes thinner. Figure 7 depicts the effect of Prandtl number (Pr) on the velocity, temperature and concentration profiles. Pr is seen to decrease the velocity and temperature profile simultaneously. Physically, the result in figure 7 is possible because fluids with greater Pr posses high viscosity and thus decelerates

Vol. 2, No. 1, June 2018
ISSN: 2616-1303 | **Web:***www.cjpas.fulokoja.edu.ng*

slowly. This result is responsible for cooling of the plate. Upon increase in Pr, a decrease of the thermal boundary layer thickness and temperature within the boundary layer is observed in figure 7. Figure 8 depicts the effect of varying permeability parameter (Ps) on the flow velocity, temperature and concentration. The flow velocity is seen in figure 8 to increase with an increase in the permeability parameter (Ps). Physically, increasing the permeability parameter expanded the porous hole and thereby gives more room for flow of fluid particles. As a result of this, the fluid moves faster within the boundary layer, thus increases the flow velocity and thicken the boundary layer. Increasing the permeability parameter does not have any effect or negligible on the temperature and concentration profile as shown in figure 8.

Figure 9 exhibit the effect of radiation parameter (Rd) on the flow velocity, temperature and concentration. As a result of increasing the radiation parameter, the hydrodynamic boundary layer thickness increases. In addition, the thermal condition of the fluid intensify as a result of increasing Rd. Increasing the thermal radiation increases the flow velocity in figure 9. This is expected because thermal radiation enhances convective flow. The thermal boundary layer increases as the thermal radiation parameter increases. As a result of this, when increasing the radiation parameter both the velocity and temperature profiles increases. Figure 10 illustrates the influence of chemical reaction parameter on the flow velocity, temperature and concentration. The rate of chemical reaction within the specie concentration is destructive. As a result of this, it reduces the solutal boundary layer. However, in the case of constructive reaction $K_c < 0$ the solutal boundary layer increases while in the case of destructive reaction $K_c > 0$, the solutal boundary layer decreases as shown in figure 10. When increasing the chemical reaction parameter, there is a slight decrease in the velocity profile but negligible on the temperature profile as shown in figure 10. The effect of Lewis number (Ln) on the flow velocity, temperature and concentration is illustrated in figure 11. Increasing Ln decreases the velocity and concentration as shown in figure 11. Increasing Ln decreases the velocity and concentration as shown in figure 11 because a very large value of the Lewis number (Ln) results to a weak molecular diffusivity and thinner boundary layer thickness. The effect of the Lewis number is negligible on the temperature profile.

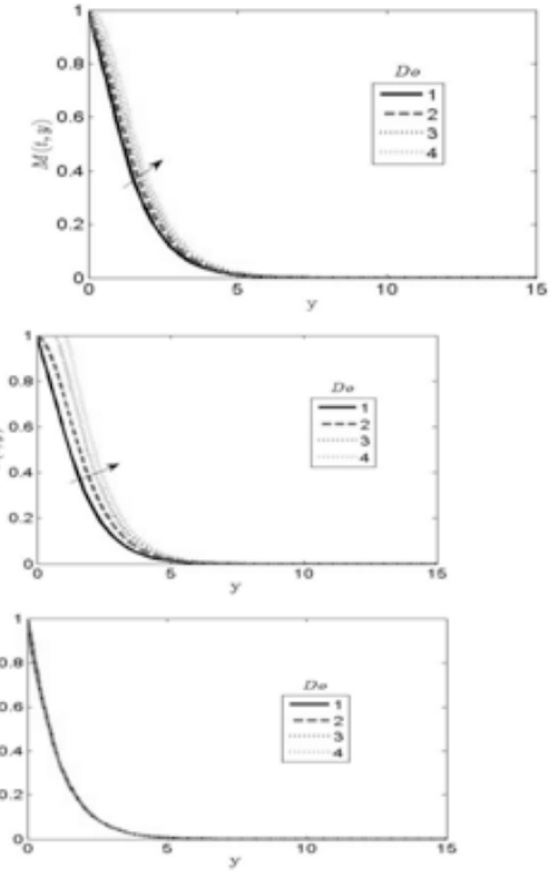

Figure 2: Effect of Do on the velocity, temperature and concentration profiles

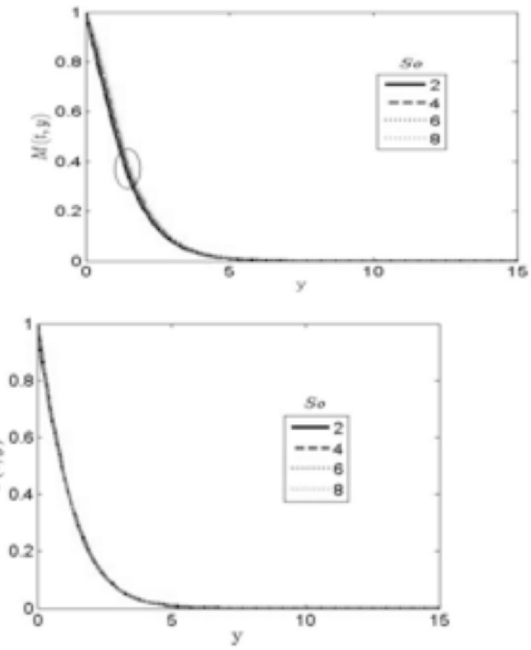

Vol. 2, No. 1, June 2018
ISSN: 2616-1303 | **Web:***www.cjpas.fulokoja.edu.ng*

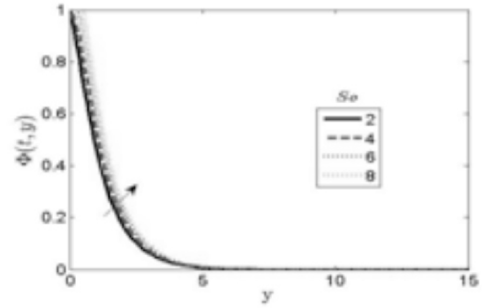

Figure 3: Effect of So on the velocity, temperature and concentration profiles

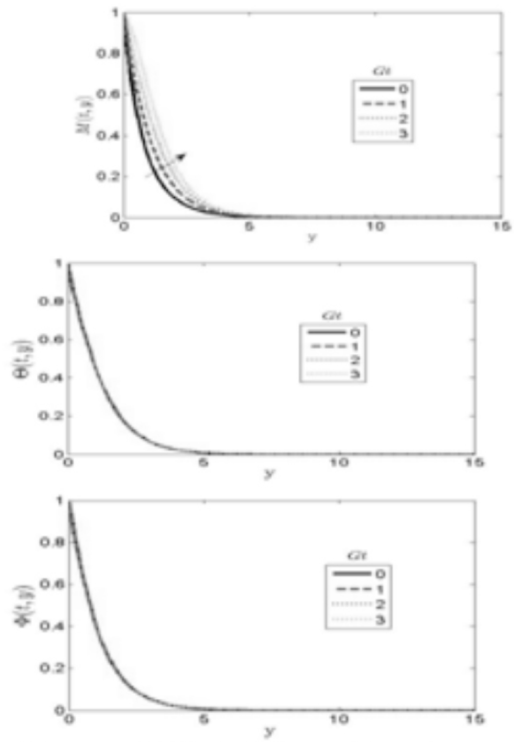

Figure 4: Effect of G_t on the velocity, temperature and concentration profiles

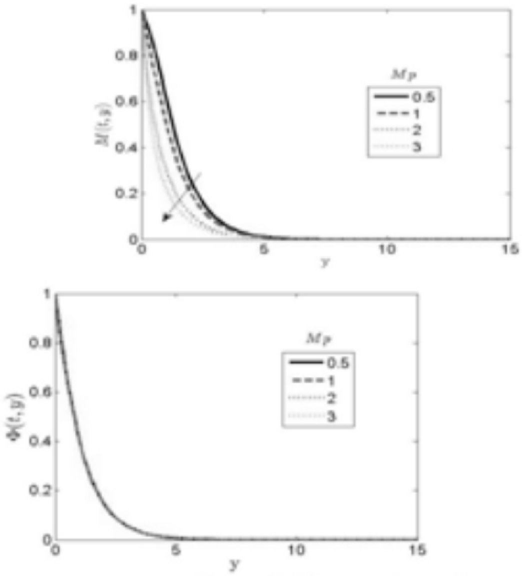

Figure 5: Effect of M_p on the velocity, temperature and concentration profiles

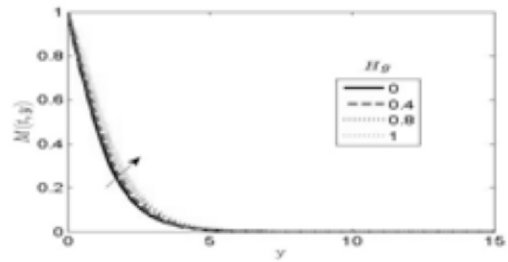

Figure 6: Effect of Hg on the velocity

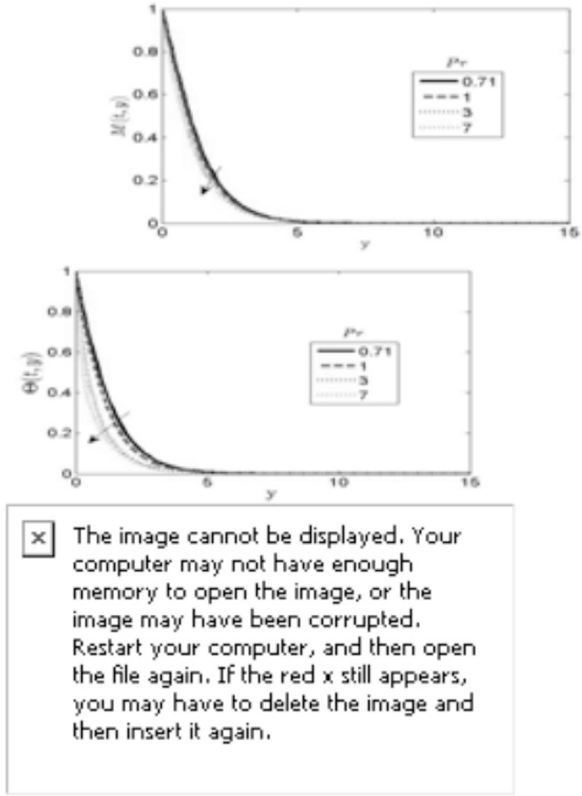

Figure 7: Effect of Pr on the velocity, temperature and concentration profiles

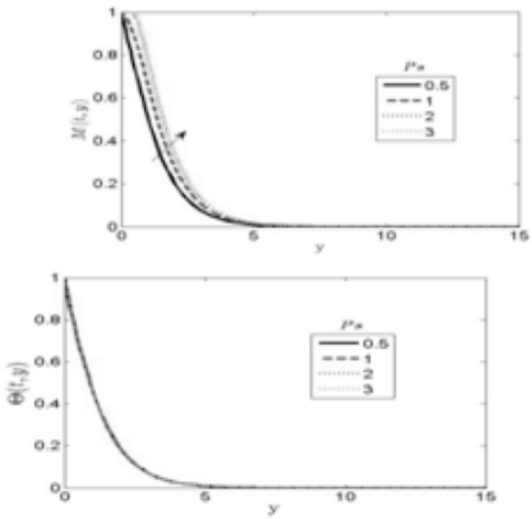

Vol. 2, No. 1, June 2018
ISSN: 2616-1303 | **Web:***www.cjpas.fulokoja.edu.ng*

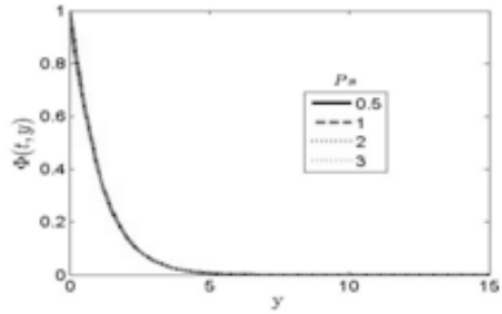

Figure 8: Effect of Ps on the velocity, temperature and concentration profiles

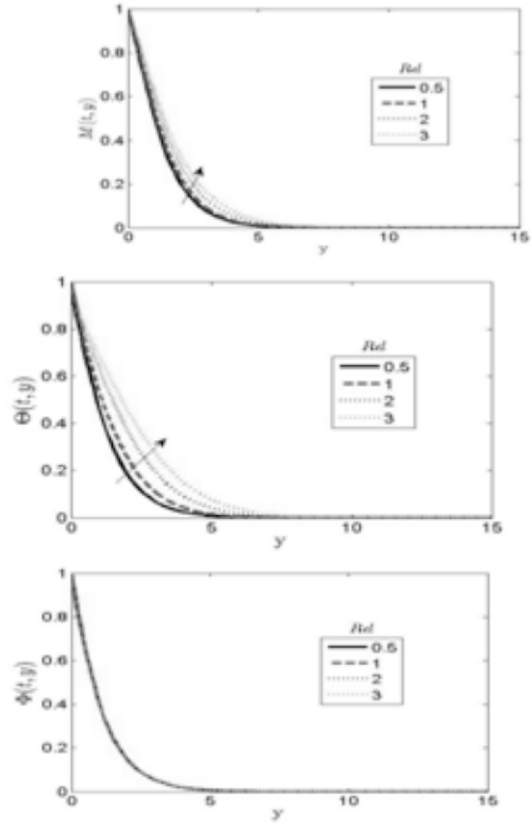

Figure 9: Effect of Rd on the velocity, temperature and concentration profiles

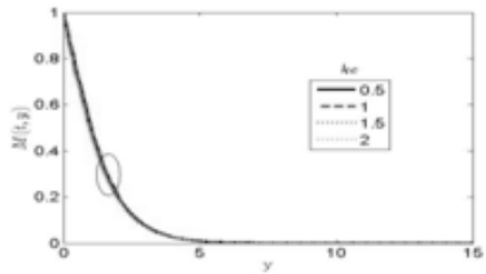

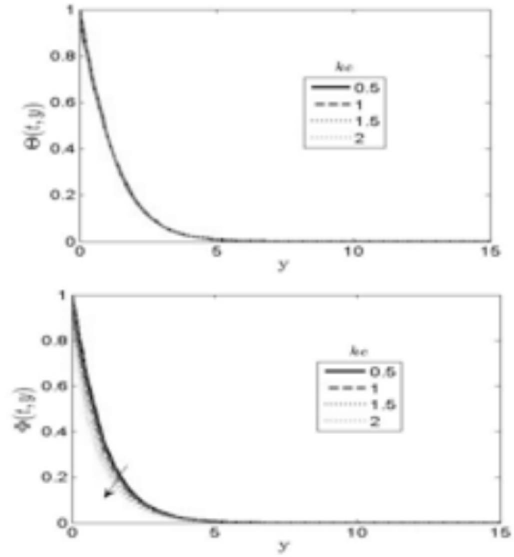

Figure 10: Effect of K_c on the velocity, temperature and concentration profiles

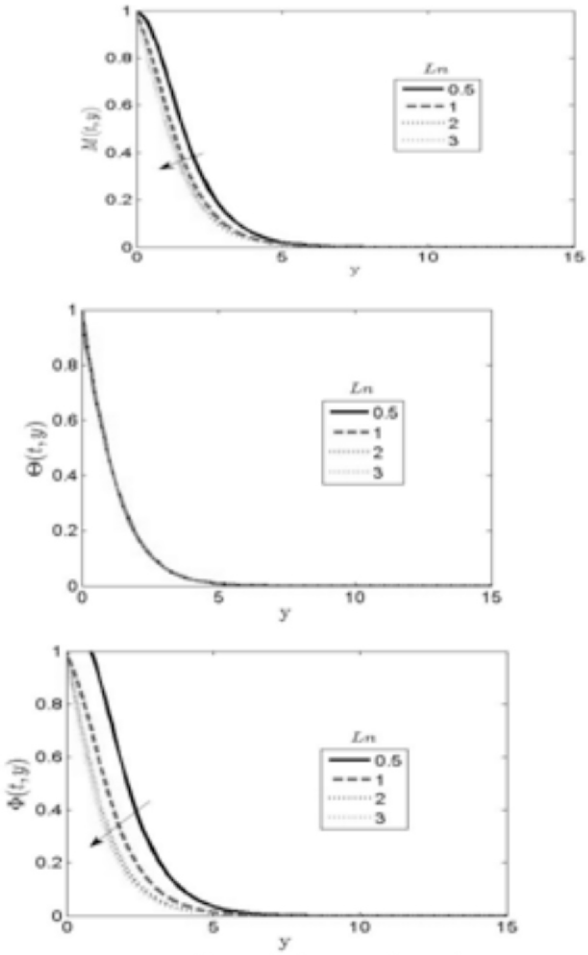

Figure 11: Effect of Ln on the velocity, temperature and concentration profiles

5. Conclusion

This paper provides the numerical solution of electrically conducting and nanofluid flow over a semi-infinite vertical porous plate with Soret-Dufour effects. The study is specifically motivated by the wide range of nanofluids heat and mass transfer applications in sciences and engineering. The main findings are as follows:

(i) The Lewis number (Ln) was seen to decelerate the velocity and concentration profiles as its value increases.
(ii) The chemical reaction within the specie concentration is seen to be destructive as its reduces the solutal boundary layer.
(iii) Increase in the permeability parameter (Ps) increases the flow velocity.
(iv) The thermal boundary layer thickness and the temperature within the boundary decreases as the value of the Prandtl number increases.

6.0References

Adegbie K.S. and Fagbade A.I. (2015):Influence of variable fluid properties and radiative heat loss on Magnetohydrodynamic forced convection flow in a fluid saturated porous medium. Journal of Nigerian Association of Mathematical Physics; 30, 101-117.

Ahmad S., Farooq M., Javed M., Aisha Anjum (2018):Double stratification effects in chemically reactivesqueezed Sutter by fluid flow with thermal radiation and mixed convection, Results in Physics, 8, 1250–1259.

Alao F.I., Fagbade A.I., Falodun B.O. (2016):Effects of thermal radiation, Soret and Dufour on an unsteadyheat and mass transfer flow of a chemically reacting fluid past a semi-infinite vertical plate with viscous dissipation,Journal of the Nigerian Mathematical Society, 35, 142–158.

Biswas R., Afikuzzaman M., Mondal M., Ahmmed S.F. (2018):MHD Free Convection and Heat Transfer Flow Through a Vertical Porous Plate in the Presence of Chemical Reaction,Frontiers in Heat and Mass Transfer (FHMT), 11, 13, DOI: 10.5098/hmt.11.13.

Durga Prasad P., Kiran Kumar R.V.M.S.S., Varma S.V.K. (2018):Heat and mass transfer analysis for the MHD flow of nanofluid with radiation absorption, Ain Shams Engineering Journal, 9, 801–813.

Ganga B., Mohamed S., Yusuff Ansari , Vishnu Ganesh N., Abdul Hakeem A.K. (2016):MHD flow of Boungiorno model nanofluid over a vertical plate with internal heat generation/absorption, Propulsion and Power Research, 5(3), 211–222.

Idowu A. S. and Falodun B. O. (2019):Soret–Dufour Effects on MHD Heat and Mass Transfer of Walter's-BViscoelastic Fluid over a Semi-Infinite Vertical Plate: Spectral Relaxation Analysis, Journal of Taibah University for Sciencehttps://doi.org/10.1080/16583655.2018.1523527.

Jithender Reddy G., Srinivasa Raju R., Manideep P., Anand Rao J. (2016):Thermal diffusion and diffusion thermo effects on unsteady MHD fluid flow past a moving vertical plate embedded in porous medium in the presence of Hall current and rotating system, Transactions of A. Razmadze Mathematical Institute, 170, 243–265.

Kalidas Das (2015):Nanofluid flow over a non-linear permeable stretching sheet with partial slip,Journal ofthe Egyptian Mathematical Society, 23, 451–456.

Kiran Kumar R. V. M. S. S., Vinod Kumar G., Raju C. S. K., Shehzad S. A. and Varma S. V. K. (2018); Analysis of Arrhenius activation energy in magnetohydrodynamic Carreau fluid flow through improved theory of heat diffusion and binary chemical reaction,Journal of Physics Communications, 2, 035004

Misra J.C., Adhikary S.D. (2016):MHD oscillatory channel flow, heat and mass transfer in a physiological fluid in presence of chemical reaction,Alexandria Engineering Journal, 55, 287–297.